

See discussions, stats, and author profiles for this publication at: <https://www.researchgate.net/publication/231681563>

Thermal Stability Study of Self-Assembled Monolayers on Mica

ARTICLE *in* LANGMUIR · MARCH 2000

Impact Factor: 4.46 · DOI: 10.1021/la990648t

CITATIONS

30

READS

9

4 AUTHORS, INCLUDING:



Bernardo R A Neves

Federal University of Minas Gerais

82 PUBLICATIONS 1,180 CITATIONS

SEE PROFILE



Phillip E. Russell

Appalachian State University

90 PUBLICATIONS 813 CITATIONS

SEE PROFILE

Thermal Stability Study of Self-Assembled Monolayers on Mica

B. R. A. Neves,[†] M. E. Salmon,[‡] P. E. Russell,^{*,‡} and E. B. Troughton, Jr.[§]

Departamento de Fisica, ICEx, UFMG, Av. Antonio Carlos, 6627, Belo Horizonte, CEP 30123-970, Brazil, Analytical Instrumentation Facility, North Carolina State University, Box 7531, Raleigh, North Carolina 27695, and Thomas Lord Research Center, Lord Corporation, 110 Lord Drive, Box 8012, Cary, North Carolina 27512

Received May 26, 1999. In Final Form: February 3, 2000

In this Letter, we report on the use of atomic force microscopy to study the thermal stability of self-assembled monolayers (SAM) of octadecylphosphonic acid (OPA) grown on mica. The samples were sequentially annealed for 30 min steps at temperatures ranging from 50 to 200 °C. A major change in the SAM morphology takes place at temperatures ~95 °C, with the disappearance of the original flat-topped and partial-coverage SAM morphology. Concomitantly, the nucleation and growth of OPA precipitates in the investigated temperature range are observed. Two separate regimes are identified: initially, for temperatures up to ~110 °C, nucleation of OPA precipitates occurs, increasing their number density. Then, for temperatures above ~10 °C, growth of OPA precipitate size dominates, with the density of precipitates remaining approximately constant. A simple model used to fit the experimental data of both regimes enables an estimate of ~9 kcal/mol as the energy required for the disorganization (E_d) of OPA molecules on mica.

In recent years, much attention has been devoted to the study of self-assembled monolayers (SAMs) and multilayers of organic materials due to their numerous potential applications as, for example, lubricants, corrosion inhibitors, or adhesion promoters.^{1,2} The most commonly studied systems consist of various types of alkanethiols deposited on gold surfaces.^{3–5} However, there are various other classes of materials which also form SAMs, enlarging the possibilities of tailoring surface properties and, thereby, controlling desired macroscopic properties of the system.^{6–8} Furthermore, there are various application methods and processing conditions that might be useful for the preparation of SAMs.

The various methods of application that can be used to form SAMs include immersion coating, spread coating, and vapor phase methods, which are of importance to many industrial processes. Virtually forgotten due to the popularity of immersion coating, but of great industrial importance, the use of spread coating to form monolayer films was described in the early monolayer work of Hardy in (1920 and 1930s)⁹ and Zisman (1950 and 1960s)^{10–13} in

the field of lubrication in which monolayers were applied by spreading drops of oils on flat horizontal metal surfaces. Spread coating the monolayer precursor onto the substrate as in painting or adhesive applications is, in many cases, the preferred method of application. Spread coating is critical to new methods of microfabrication or “soft lithography” technology, which have been reviewed by Whitesides.¹⁴ Unfortunately, relatively little research has been published concerning monolayers applied by spread coating. Larsen¹⁵ does report that STM images of surface films of dodecanethiol attached to Au(111) formed by microcontact printing (a form of spread coating) are indistinguishable from those formed by immersion and adsorption from solutions. However, it is interesting to investigate whether surface films prepared by spread coating are similar, in general, to monolayer films prepared by immersion.

In addition, after a film is applied to a surface, the surface film may be further processed or subjected to heat, for example, to remove solvent or in some instances for the improvement of performance. Relatively little research is available to describe the structural changes in surface films of organic monolayers during solvent evaporation or processes involving heat. Thus, this paper reports on the structure of surface films prepared by spread coating and the structural changes resulting from thermal processing.

In this work, we have investigated some effects of annealing octadecylphosphonic acid $-\text{CH}_3(\text{CH}_2)_{17}-\text{PO}_3\text{H}_2-$ (OPA) monolayers deposited on mica.⁶ The OPA forms a SAM through the adsorption of the phosphorus-rich headgroup (PO_3H_2) on the surface of mica (i.e., SiO_3^-).^{6,7} Long-range forces, mainly van der Waals forces, among

[†] Departamento de Fisica, ICEx, UFMG.

[‡] Analytical Instrumentation Facility, North Carolina State University.

[§] Thomas Lord Research Center, Lord Corporation.

(1) Laibinis, P. E.; Hickman, J. J.; Wrighton, M. S.; Whitesides, G. M. *Science* **1989**, *245*, 845.

(2) Ulman, A. *An Introduction to Ultrathin Films*; Academic Press: San Diego, CA, 1991.

(3) Dubois, L. H.; Nuzzo, R. G. *Annu. Rev. Phys. Chem.* **1992**, *43*, 437.

(4) Troughton, E. B.; Bain, C. D.; Whitesides, G. M.; Nuzzo, R. G.; Allara, D. L.; Porter, M. D. *Langmuir* **1988**, *4*, 365.

(5) Delamarche, E.; Michel, B.; Kang, H.; Gerber, Ch. *Langmuir* **1994**, *10*, 4103 and references therein.

(6) Woodward, J. T.; Ulman, A.; Schwartz, D. K. *Langmuir* **1996**, *12*, 3626.

(7) Woodward, J. T.; Schwartz, D. K. *J. Am. Chem. Soc.* **1996**, *118*, 7861.

(8) Richards, J. F. MSc Thesis; North Carolina State University, Raleigh, NC, 1997.

(9) Hardy, W. B. *Collected Scientific Papers*; Cambridge University Press: 1936.

(10) For a discussion of the spreading of drops of oils on flat horizontal metal surfaces, see pages 533–534 of: Bigelow, W. C.; Pickett, D. L.; Zisman, W. A. *J. Colloid Sci.* **1946**, *1*, 513–538.

(11) Levine, O.; Zisman, W. A. *J. Phys. Chem.* **1957**, *61*, 1068–1077.

(12) Levine, O.; Zisman, W. A. *J. Phys. Chem.* **1957**, *61*, 1118–1196.

(13) Adamson, A. W. *Physical Chemistry of Surfaces*, 4th ed.; John Wiley & Sons: New York, 1982; p 173.

(14) Microcontact printing is a process forming SAMs by transfer of adsorbate solutions from the surfaces of patterned stamps to metals. See page 558 of: Xia, Y.; Whitesides, G. M. *Angew. Chem., Int. Ed. Engl.* **1998**, *37*, 550–575.

(15) Larsen, N. B.; Biebuyck, H.; Delamarche, E.; Michel, B. *J. Am. Chem. Soc.* **1997**, *119*, 3017–3026.

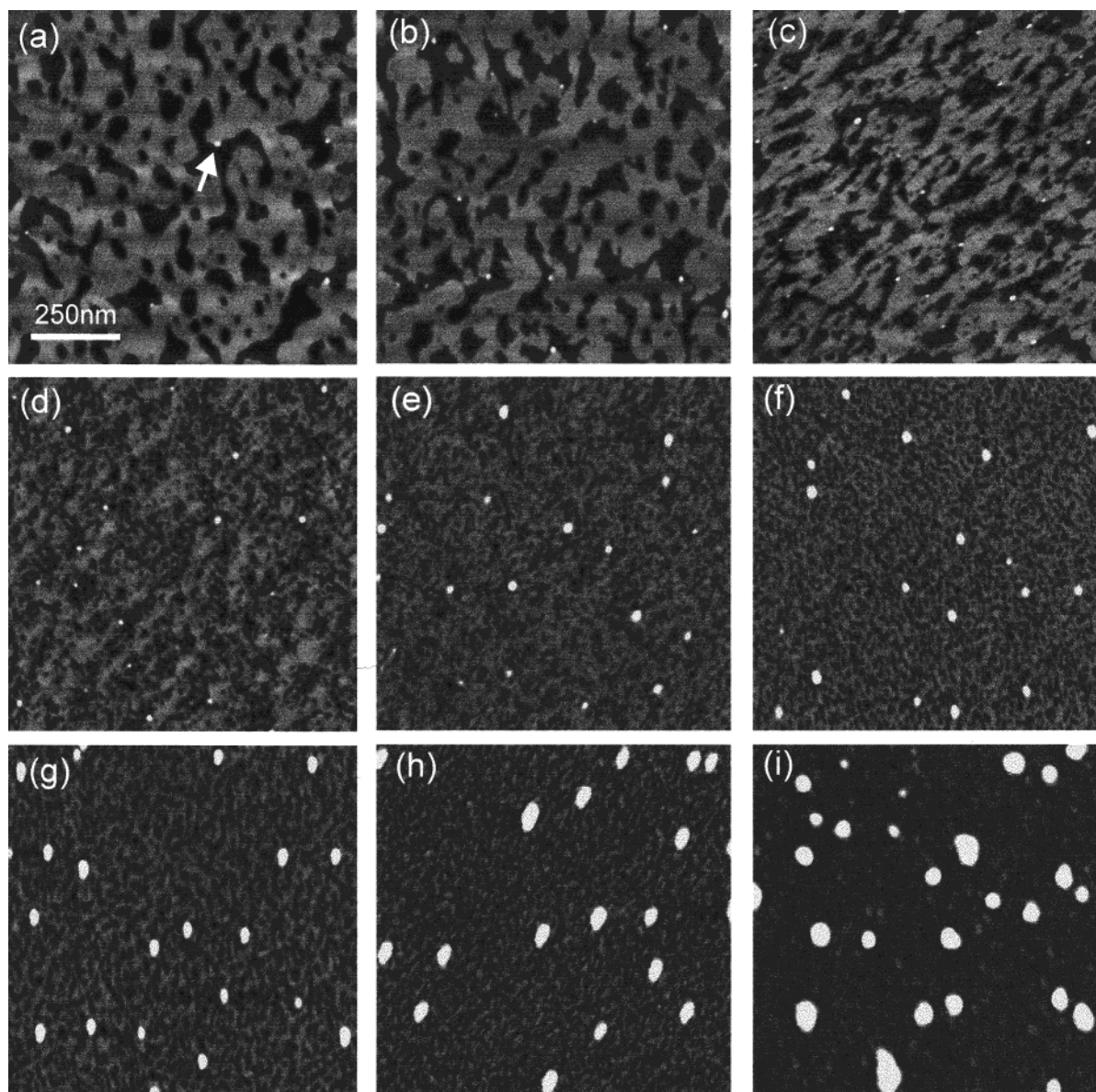


Figure 1. Series of AFM images of a sample surface after preparation and after annealing at 80, 90, 100, 110, 120, 140, 180, and 200 °C (from panels a to i, respectively). All images are $1\ \mu\text{m} \times 1\ \mu\text{m}$. The arrow in panel a indicates the location of a precipitate.

the carbon chains drive the monolayers into spatial organization. Possible H-bonding of PO_3H_2 to mica surfaces (i.e., SiO_3^-) may be also partially responsible for the self-assembly mechanism. Molecular resolution images taken with atomic force microscopy (AFM) show that the OPA surface structure follows the underlying hexagonal structure of the mica surface.⁸ The sample preparation procedure is very simple and easily reproducible: a droplet of an OPA solution is laid on a freshly cleaved mica surface and allowed to spread. After typically a few seconds, dewetting of the OPA solution on mica takes place and almost all of the adsorption solution spreads off the mica surface. Ultrapure (99.99%) nitrogen is used to blow-dry the rest of the adsorption solution from the sample holder. In the present study, we have used a 0.1 wt % solution of OPA dissolved in absolute ethanol (which corresponds to a 2.1 mM solution) to prepare the samples.

Imaging data were recorded for samples that were annealed for 30 min at temperatures ranging from 50 to 200 °C, with 10 °C sequential steps using a conventional oven at ambient pressure. After each annealing step, the samples were imaged by AFM (Digital Instruments MultiMode SPM) operating in TappingMode at room

temperature and then returned to the oven for another thermal treatment. Several (5–10) images were acquired at different regions to assess the homogeneity along the surface of the samples. The samples were found to be homogeneous over the observed scale of these AFM experiments (up to $5\ \mu\text{m} \times 5\ \mu\text{m}$, for each image). For each region, two images of different sizes were acquired in order to investigate any possible damages to the sample surface caused by the imaging process and also to enhance the quality of OPA precipitate statistics in each case reported. First, a $1\ \mu\text{m} \times 1\ \mu\text{m}$ image was acquired, recording detailed morphology information, and then a $3\ \mu\text{m} \times 3\ \mu\text{m}$ image was obtained, allowing for damage investigation and better statistical analysis.

Figure 1 presents a summary of all the modifications in the morphology of the OPA/mica system as a function of the annealing temperature. A series of $1\ \mu\text{m} \times 1\ \mu\text{m}$ images shows the typical morphology of the sample surface with no annealing and after annealing at the temperatures of 80, 90, 100, 110, 120, 140, 180, and 200 °C (panels a–i of Figure 1, respectively). Figure 1a (no annealing) shows the mica surface (dark regions in the figure) partially covered ($\sim 70\%$) by the OPA monolayer (gray regions). The

average height of the OPA monolayer is found to be 1.65 nm, which indicates a tilt angle of $\sim 46^\circ$ between the OPA molecule and the surface normal vector, which is in good agreement with previous works.^{6,8} It is important to note that the partial coverage of the monolayer in Figure 1a is possibly due to short (5–10 s) adsorption times constituting an interrupted growth process. There is also some evidence that water might also be playing a role in the adsorption process, creating a competition with the OPA molecules for mica binding sites. The presence of water may be an important factor while imaging the deposited films in ambient using TappingMode.^{16,17} In contrast to the partial coverage exhibited by spread or drip coatings, coverage of 99% completion has been seen using in situ AFM studies of immersed samples.⁸

Carefully inspecting Figure 1a, one can see a few white dots (high spots) located at some OPA/mica edges (one of them is indicated by an arrow in Figure 1a). These dots are believed to be OPA precipitates, or crystallites, for the following reasons: The solubility of OPA in ethanol is low, being approximately 0.1 wt % at room temperature,⁸ which is the nominal concentration of the solution used. However, at 15–20 °C, ethanolic solutions of OPA are saturated at concentrations above 0.1 wt % solution. Therefore, any small fluctuations on the solution temperature could lead to formation of these tiny (10 nm in diameter) OPA precipitates, which are then deposited, on the mica surface. However, the fact that these precipitates are always observed at the edges may indicate that they actually originate during the SAM growth.² Defects on the mica surface could also lead to nucleation of the precipitates. A detailed investigation on the origin of the precipitates is out of the scope of this work and will only be briefly discussed at the end of this Letter. However, it should be pointed out that control samples with ethanol only (no OPA), dripped on freshly cleaved mica surfaces, did not show any precipitate formation during identical annealing experiments, supporting the OPA precipitate hypothesis.

There are no major changes in the system morphology with annealing temperatures up to 80 °C, as shown in Figure 1b. Perhaps the most noteworthy difference is a pronounced increase in the number of precipitates (better seen in $3\ \mu\text{m} \times 3\ \mu\text{m}$ images, not shown in the figure). However, after annealing at 90 °C, a noticeable change in the OPA monolayer morphology is initiated as shown in Figure 1c, and there is also a further increase in the number of precipitates. This change in morphology is even more accentuated after annealing at 100 °C, as shown in Figure 1d. It is now difficult to identify the well-defined regions of OPA monolayers and mica. There are some residual regions of OPA monolayers, represented by the light gray regions in Figure 1d. These regions exhibit an average height of 0.95 nm. Perhaps the orientation of the OPA film is best described as a monolayer of OPA with a very large tilt angle ($\sim 68^\circ$) between the OPA molecules and the mica surface normal. Alternative structures may be possible that would give an average height of 0.95 nm, as for example a liquid–glass-like phase, which would still give the same image. As observed in the previous two images, an increase in the precipitate density is also observed. Going one step further in the annealing process (110 °C), the well-defined regions of OPA monolayers are no longer present in the AFM image, as shown in Figure 1e. The number density of precipitates is still increasing,

but at this temperature, the average size of the precipitates is also increasing as opposed to the previous annealing temperatures, where the sizes of precipitates remained constant and only their number increased. After annealing at 120 °C, there seems to be no further change in the overall system morphology, as shown in Figure 1f. Although a saturation in the number of precipitates is noticed, i.e., there is not a sizable increase in their number density, still further growth of precipitates, i.e., an average size increase, is observed. Above 120 °C, the only observed effect of the annealing is the growth of precipitates, with their number being kept approximately constant, as can be seen in panels g–i of Figure 1 representing annealing temperatures of 140, 180, and 200 °C, respectively.

The results shown in Figure 1 indicate that the initial morphology of the OPA monolayer on mica is stable over the temperature range from 25 to 90 °C. It is reasonable to suppose that the adsorption energy of OPA molecules on mica is quite low due to the observed breakdown of the initial film morphology along with the significant increase in the precipitate nucleation at temperatures slightly above 50 °C. The adsorption of OPA molecules on mica is weak, governed by the long-ranged van der Waals interactions between chains and H-bonding interactions between the polar phosphonic acid headgroup and the mica. Therefore, the adsorption, or decomposition, energy for this system should be much smaller than that observed for the chemisorbed alkanethiols on gold.^{1–5,18}

To make an estimation of the energy required for OPA molecule mobility, energy of disorganization (E_d), a more quantitative study on the influence of annealing temperature on the precipitate density and size was carried out. For each temperature, $3\ \mu\text{m} \times 3\ \mu\text{m}$ images were used to calculate the average number density and $1\ \mu\text{m} \times 1\ \mu\text{m}$ images were used to calculate the average radius of the precipitates. It should be noted that the precipitate radius exhibits a narrow Gaussian distribution for all images, and therefore, taking the center value of the distribution was considered a good approximation for the average radius. Although Figure 1i may seem to indicate a large size distribution, it is not the case. All the largest precipitates are actually formed by two, or more, precipitates which can be easily identified by phase contrast imaging.^{16,19} The results of density and radius of the precipitates as function of temperature are shown in parts a and b of Figure 2, respectively. In Figure 2a, a strong increase in the density of precipitates is observed over the temperature range from 50 to 110 °C, after which the density of precipitates approaches a constant level upon further increases in temperature. On the other hand, the average radius of the precipitate is constant for temperatures up to ~ 100 °C and then increases more than 5 times in the temperature range between 100 and 200 °C, as shown in Figure 2b.

The experimental data shown in figure 2 can be fit using a very simple model from which one can estimate E_d . The data can be described as having two separate regimes: one regime is the increase in precipitate density for temperatures up to ~ 110 °C, and the other regime is growth of precipitate for higher temperatures, with a small overlap of both regimes at ~ 110 °C. Initially considering the first regime, the following assumption is made: all the precipitates are formed from OPA molecules that are mobile on the mica surface. Furthermore, assuming that there is a fixed probability that a mobile molecule will

(16) Neves, B. R. A.; Leonard, D. N.; Salmon, M. E.; Troughton, E. B., Jr.; Russell, P. E. *Nanotechnology* **1999**, 10 (4), 399–404.

(17) Sauer, B. B.; McLean, R. S.; Thomas, R. R. *Langmuir* **1998**, 14 (11), 3045–3051.

(18) Atkins, P. *Physical Chemistry*; W. H. Freeman and Co.: New York, 1994.

(19) Digital Instruments, Santa Barbara, CA, 1990.

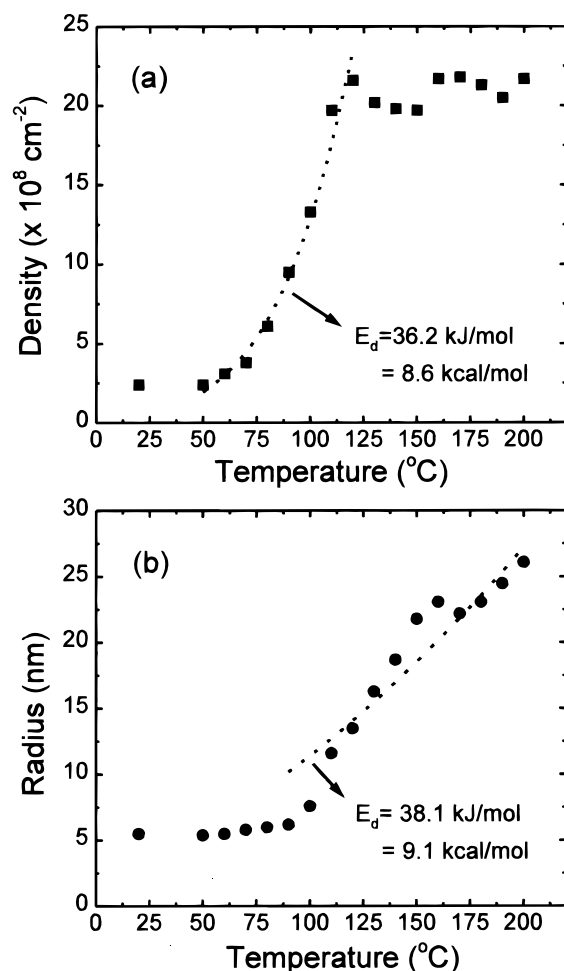


Figure 2. Graphs of the density of precipitates (a) and radius of precipitates (b) as a function of annealing temperature. The dotted line indicates the fitting with the used model and the obtained E_d values are also shown.

attach to others forming precipitates, then it is straightforward that the number density of precipitates is directly proportional to the probability of monomer diffusion. With the diffusion of monomer being a thermally activated process, it is reasonable to write the functional dependence of precipitate density d with temperature T , in K, as:¹⁸

$$d = \alpha \exp(E_d/kT) \quad (1)$$

where α is a fitting parameter, k is the Boltzmann constant, and E_d is the energy required for monomer transport and film disorganization. Equation 1 was used to fit the data in Figure 2a in the range $50 \text{ }^{\circ}\text{C} \leq T \leq 120 \text{ }^{\circ}\text{C}$, and the result is shown as a dotted line in the figure. A value of $E_d = 36.2 \text{ kJ/mol} = 8.6 \text{ kcal/mol}$ for the transport energy of the OPA molecules is found from this fitting.¹⁸

Now considering the second regime, shown in Figure 2b, and assuming the same hypothesis stated above, it is

possible to use the same model to fit the data. It has to be noticed however, assuming a volumetric growth of the precipitates, that their radius growth is proportional to the $1/3$ power of the number of mobile molecules. Therefore, it is possible to relate the radius r with temperature T , in K, as

$$r = \beta \exp(E_d/kT)^{1/3} \quad (2)$$

where β is a fitting parameter. By use of eq 2 to fit the experimental data in the range $90 \text{ }^{\circ}\text{C} \leq T \leq 200 \text{ }^{\circ}\text{C}$ (dotted line in Figure 2b), $E_d = 38.1 \text{ kJ/mol} = 9.1 \text{ kcal/mol}$. The 5% difference between the two obtained values for E_d is within the experimental errors, and it can be concluded that there is only one activation energy for both regimes within the entire studied temperature range. This means that the change in regimes (precipitate nucleation versus precipitate growth) is not explained by different diffusion processes with different characteristic energies. This phenomenon of initial island nucleation, with fixed size, followed by island growth, with no further nucleation, resembles the Stransky–Krastanov (SK) mode of growth (intensely studied in InAs/GaAs and Ge/Si systems for example^{18,19}). In the SK mode of growth, after deposition of a primary layer, the islands initially grow coherently, i.e., with an optimum size, which is defined by surface energy considerations (mainly due to stress and strain).^{20,21} The increasing amount of the growing species which causes the transition from one growth regime to another in normal SK systems has an analogous temperature profile in the present case: as the temperature is increased, more OPA molecules will become thermally mobile and available for precipitate nucleation and/or growth. A recent study on annealing effects on the morphology of Ge islands on Si showed a coarsening effect, i.e., the large islands become even larger at the expense of material coming from smaller islands, which then disappear.²¹ Although this Ostwald ripening process²¹ could be possible in the present system, it should normally lead to a decrease in precipitate density, which was not observed. Longer annealing times may be needed for the observation of the coarsening effect.²¹ Taking all the above into consideration, it is clear that a detailed study on the origin of both regimes found in the present work is still needed and is considered a natural step forward in the investigation of this system.

In conclusion, an AFM study on the thermal stability of OPA self-assembled monolayers grown on mica has been presented. Partial monolayer films formed by spread coating were similar in structure to partial monolayer films prepared by immersion coating.²² The monolayer films were not strongly attached to the mica, and upon heating, the initial monolayer morphology became disorganized and the mobile molecules migrated across the surface of the mica forming large precipitates. It was possible to clearly identify a large morphology change in the system utilizing an annealing temperature range between 90 and 110 $^{\circ}\text{C}$. Nucleation and growth of precipitates, which originate from thermally mobile OPA molecules on the mica surface, have also been observed. A simple model used to fit the experimental data enabled an estimate of the energy of disorganization, for the OPA/mica system.

LA990648T

(20) Neves, B. R. A.; Andrade, M. S.; Rodrigues, W. N.; Sáfar, G. A. M.; Moreira, M. V. B.; de Oliveira, A. G. *Appl. Phys. Lett.* **1998**, *72*, 1712.

(21) Kamins, T. I.; Medeiros-Ribeiro, G.; Ohlberg, D. A. A.; Stanley Williams, R. J. *Appl. Phys.* **1999**, *85*, 1159.

(22) Woodward, J. T.; Dondevski, I. *J. Phys. Chem. B* **1997**, *101*, 7535–7541.